Forkhead Domain Inhibitor-6 Suppresses Corneal Neovascularization and Subsequent Fibrosis After Alkali Burn in Rats

Chunlin Lan,[1] Guo Liu,[2] Longxiang Huang,[1] Xizhen Wang,[3] Junkai Tan,[4] Yun Wang,[3] Ning Fan,[3] Yihua Zhu,[1] Man Yu,[5,6] and Xuyang Liu[4,7]

[1]The First Affiliated Hospital of Fujian Medical University, Fuzhou, Fujian, China
[2]Sichuan Provincial Key Laboratory for Human Disease Gene Study, Sichuan Provincial People's Hospital, University of Electronic Science and Technology of China, Chengdu, Sichuan, China
[3]Shenzhen Key Laboratory of Ophthalmology, Shenzhen Eye Hospital, Jinan University, Shenzhen, Guangdong, China
[4]Xiamen Eye Center, Xiamen University, Xiamen, Fujian, China
[5]Department of Ophthalmology, Sichuan Provincial People's Hospital, University of Electronic Science and Technology of China, Chengdu, Sichuan, China
[6]Research Unit for Blindness Prevention of Chinese Academy of Medical Sciences (2019RU026), Sichuan Academy of Medical Sciences, Chengdu, Sichuan, China
[7]Department of Ophthalmology, Shenzhen People's Hospital, the 2nd Clinical Medical College, Jinan University, Shenzhen, China

Correspondence: Xuyang Liu, Xiamen Eye Center, Xiamen University, Xiamen Ophthalmology Department Center Building, Xiahe Road No. 336, Xiamen, Fujian, China; xliu1213@126.com.
Man Yu, Department of Ophthalmology, Sichuan Provincial People's Hospital, University of Electronic Science and Technology of China, Chengdu, Sichuan 610072, China; yuman712@126.com.
Yihua Zhu, The First Affiliated Hospital of Fujian Medical University, Bayiqi Middle Road No. 15 Nearby, Fuzhou, Fujian, China; Zhuyihua209@163.com.

CL, GL, LH, and XW contributed equally to this paper.

Received: December 11, 2021
Accepted: March 27, 2022
Published: April 21, 2022

Citation: Lan C, Liu G, Huang L, et al. Forkhead domain inhibitor-6 suppresses corneal neovascularization and subsequent fibrosis after alkali burn in rats. *Invest Ophthalmol Vis Sci.* 2022;63(4):14. https://doi.org/10.1167/iovs.63.4.14

Purpose. The purpose of this study was to investigate the effects of Forkhead Domain Inhibitor-6 (FDI-6) on regulating inflammatory corneal angiogenesis and subsequent fibrosis induced by alkali burn.

Methods. A corneal alkali burn model was established in Sprague Dawley rats using NaOH and the rat eyes were topically treated with FDI-6 (40 µM) or a control vehicle four times daily for 7 days. Corneal neovascularization, inflammation and epithelial defects were observed on days 1, 4, and 7 under a slit lamp microscope after corneal alkali burn. Analysis of angiogenesis-, inflammation-, and fibrosis-related indicators was conducted on day 7. Murine macrophages (RAW264.7 cells) and mouse retinal microvascular endothelial cells (MRMECs) were used to examine the effects of FDI-6 on inflammatory angiogenesis in vitro.

Results. Topical delivery of FDI-6 significantly attenuated alkali burn-induced corneal inflammation, neovascularization, and fibrosis. FDI-6 suppressed the expression of angiogenic factors (vascular epidermal growth factor, CD31, matrix metalloproteinase-9, and endothelial NO synthase), fibrotic factors (α-smooth muscle actin and fibronectin), and pro-inflammatory factor interleukin-6 in alkali-injured corneas. FDI-6 downregulated the expression of monocyte chemotactic protein-1, pro-inflammatory cytokines (interleukin-1β and tumor necrosis factor-alpha), nucleotide-binding oligomerization domain-like receptor family pyrin domain-containing 3, and vascular endothelial growth factor in RAW264.7 cells and inhibited the proliferation, migration, and tube formation of MRMECs in vitro.

Conclusions. FDI-6 can attenuate corneal neovascularization, inflammation, and fibrosis in alkali-injured corneas.

Keywords: corneal neovascularization, corneal inflammation, corneal fibrosis, forkhead box M1 (FOXM1), forkhead domain inhibitor-6 (FDI-6)

Corneal neovascularization (corneal NV), characterized by the formation of new capillary blood vessels from the limbus toward the center of the cornea, is a sight-threatening ocular disorder that affects more than 1.4 million people.[1] Corneal NV is a type of pathological neovascularization that can cause corneal edema or opacity, leading to poor corneal transparency.[2] Until now, treatment options for corneal NV, including topical steroids, anti-inflammatory drugs, and anti-VEGF inhibitors, have remained the mainstay of treatment; however, significant side effects, drug resistance, and limited efficacy are still major issues.[1,3,4] Accordingly, there is an urgent need to develop novel therapeutic drugs against corneal NV.

It is widely acknowledged that corneal NV is a complex pathological process that involves interactions among multiple cells, such as vascular endothelial cells (ECs),

inflammatory cells and fibroblasts, and the mutual regulation between pro-angiogenic and antiangiogenic factors.[5–7] Corneal inflammation can occur upon exposure to the immunogen, chemical burn, trauma, or infection, leading to the recruitment of neutrophils and macrophages that secrete numerous proangiogenic factors (VEGF, matrix metalloproteinases [MMPs], and fibroblast growth factor [FGF]) and profibrotic factors (transforming growth factor-β [TGF-β] and α-smooth muscle actin [α-SMA]), promote corneal NV and subsequent corneal fibrosis, which is considered one of the major factors responsible for angiogenesis.[8,9] Given their critical role in corneal NV, ECs proliferate, migrate, and generate new blood vessels in an inflammation-dependent or independent manner, and their inhibition is one of the main therapeutic strategies in neovascular diseases.[10] Preclinical studies have shown that combination and multiple target approaches have become the focus of antivascular strategies or normalization of the tumor vasculature.[11,12] Therefore, simultaneously targeting ECs, inflammatory cells, and fibroblasts may be a promising strategy for treating corneal NV.

Forkhead box M1 (FOXM1), a member of the Forkhead Box (Fox) family, is recognized as a critical proliferation-related transcription factor in cell cycle progression, DNA damage repair, and other biological processes.[13] FOXM1 overexpression has been associated with the initiation and progression of neovascular diseases (tumor angiogenesis[14]), inflammatory conditions (pneumonia,[15] osteoarthritis,[16] and liver inflammation[17]) and fibrotic diseases (idiopathic pulmonary fibrosis,[18] renal fibrosis,[19] and glaucoma filtering surgery associated fibrosis[20]). In contrast, the suppression of FOXM1 expression can decrease the expressions of molecules in FOXM1-associated pathways and further improve disease pathology.[14–20] Forkhead Domain Inhibitor-6 (FDI-6; NCGC00099374), a specific inhibitor of FOXM1, has been reported to exert an antitumor effect by inhibiting cancer cell survival, proliferation, and tumor angiogenesis.[21,22] Our previous study found that FDI-6 can bind directly to FOXM1, prevent FOXM1 from binding to its genomic target, suppress TGF-β1-induced ECM proteins synthesis, myofibroblast activation, cellular proliferation, and migration in cultured rabbit tenon's fibroblasts in vitro and attenuate subconjunctival fibrosis secondary to trabeculectomy in vivo.[20] Moreover, infiltration of a number of inflammatory cells into the conjunctival epithelium caused by trabeculectomy was also alleviated by FDI-6 treatment.[20] To the best of our knowledge, no study has previously investigated the role of FDI-6 in ocular neovascularization.

In the present study, we investigated the inhibitory effects of FDI-6 on the biological activity of mouse retinal microvascular endothelial cells (MRMECs) and lipopolysaccharide (LPS)-stimulated murine macrophages (RAW264.7 cells) in vitro and inflammatory corneal NV and fibrosis using an alkali burn-induced rat model in vivo. Our results suggest that FDI-6 holds promising potential as an antiangiogenic agent for inflammatory corneal NV.

Materials and Methods

Animals

Adult Sprague Dawley (SD; 15 males and 15 females, 6–8 weeks, 180–220 g) rats were purchased from the Institute of Laboratory Animal Sciences, Sichuan Academy of Medical Sciences, Chengdu, China. Animal studies were conducted in accordance with the Association for Research in Vision and Ophthalmology (ARVO) statement for the Use of Animals in Ophthalmic and Vision Research and approved by the Institutional Animal Care and Use Committee of the Institute of Laboratory Animal Sciences, Sichuan Academy of Medical Sciences and Sichuan Provincial People's Hospital.

Alkali Burn-Induced Corneal Neovascularization Model and FDI-6 Treatments. An animal model of corneal neovascularization induced by alkali burn was established as previously described.[8] Briefly, rats were anesthetized with an intraperitoneal injection of 10% chloral hydrate (0.4 mL/100 g) and given a drop of 0.5% tetracaine solution (Zhongshan Ophthalmic Center, Sun Yat-Sen University, Guangzhou, China) for topical anesthesia of the ocular surface before operation. Under an ophthalmic surgical microscope, a 3.5 mm filter paper soaked in 1N NaOH was gently placed on the central cornea of the right eye for 45 seconds, then the right cornea was rinsed with 30 mL of saline for 1 minute. The right eye of each rat underwent corneal alkali burn and the left eye served as a control. Both rat eyes received a 20 µL subconjunctival injection of FDI-6 (40 µM; Sigma Aldrich, St. Louis, MO, USA) or saline on the day of the operation. Then, a drop of FDI-6 was topically applied to rat eyes 4 times daily for 7 days. A 40-µM dose was selected based on a preliminary study that demonstrated that corneal NV was inhibited without adverse side effects at this dose. An experienced ophthalmologist performed all treatments.

All rats were randomly divided into 4 groups (N = number of animals; 15 eyes per group) and treated as follows: (1) saline-only group; (2) FDI-6 (40 µM)-only group; (3) saline + burn group; and (4) FDI-6 (40 µM) + burn group. FDI-6 was dissolved in dimethyl sulfoxide (DMSO), whereas saline also contained 0.17% DMSO.

Slit-Lamp Microscopic Examination. All rat eyes were evaluated under a slit lamp microscope at days 1, 4, and 7 post-alkali injury. The degree of corneal epithelial defect was assessed with 0.1% fluorescein sodium staining under a cobalt blue filter. As described previously,[23] the area of corneal NV was calculated using the following formula: $S = C/12 \times 3.1416 \times [r^2 - (r - I)^2]$, (S = the area of corneal NV, C = clock hours, r = the radius of the cornea, and I = vessel length measured from the limbus), and all the above parameters were measured using ImageJ software. The degree of corneal inflammation, corneal edema, and corneal opacity was graded using an inflammatory index, as previously described.[24,25]

Histopathologic Examination. Hematoxylin and eosin (H&E) stainings were performed to detect the histopathological changes in alkali burned corneas with or without FDI-6 treatment. All rats were euthanized with an overdose of anesthesia at day 7 post-alkali burn, and both eyes were immediately enucleated and fixed in formaldehyde, acetic acid, and saline (FAS) fixative (Wuhan Servicebio, Wuhan, China) for 48 hours. The eyes were then embedded in paraffin, cut into sequential 4-µm tissue sections, and dewaxed with xylene. These sections were analyzed by H&E staining for pathological analysis and Masson's trichrome staining for assessing the degree of the collagen volume fraction (CVF). The degree of corneal fibrosis was determined according to the following formula: CVF = collagen area/total area × 100%.

Immunohistochemistry Analysis. Immunohistochemistry analysis was performed to assess neovascularization

zation- and fibrosis-related molecular marker expression changes associated with corneal alkali burn upon FDI-6 treatment. Each eyeball section was prepared as mentioned above and blocked with 10% goat serum at room temperature (RT) for 30 minutes. Then, these sections were conjugated at 4°C overnight with the following primary antibodies: FOXM1 (ab207298, rabbit monoclonal antibody, 1:1,000; Abcam, Cambridge, MA, USA), CD31 (ab9498, mouse monoclonal antibody, 1:500; Abcam, Cambridge, MA, USA), and α-SMA (ab7817, mouse monoclonal antibody, 1:500; Abcam, Cambridge, MA, USA), and further conjugated with peroxidase-conjugated secondary antibodies at RT for 1 hour. Finally, sections were visualized using 3, 3′-diaminobenzidine (DAB) and counterstained with hematoxylin.

Immunofluorescent and TUNEL Analysis. Immunofluorescent and TUNEL analyses were performed to assess the changes in expression of inflammation- and apoptosis-related molecular marker associated with corneal alkali burn following FDI-6 treatment. Sections of each eyeball were prepared as mentioned above. For immunofluorescence staining, sections were blocked with 3% BSA at RT for 1 hour and incubated at 4°C overnight with anti-CD163 antibody (ab87099, rabbit monoclonal antibody, 1:1,000; Abcam). Then, these sections were incubated with Alexa Fluor 594 donkey anti-rabbit (A201207, 1:1000; Invitrogen, Carlsbad, CA, USA) and further counterstained with DAPI for 3 minutes (F6057-20ML, Sigma Aldrich). For TUNEL staining, sections were processed with a TUNEL kit (11684817910; Roche, Basel, Switzerland) according to the product manual and further counterstained with DAPI for 3 minutes.

Cells were fixed with 4% PFA at RT for 10 minutes and further incubated with 3% BSA and 0.5% Triton X-100 at RT for 1 hour. For CD163 staining, cells were incubated at 4°C overnight with anti-CD163 antibody, then incubated with Alexa Fluor 594 donkey anti-rabbit. For F-actin staining, cells were incubated with Rhodamine-phalloidin (PHDR1, 1:150; Cytoskeleton, Denver, CO, USA) at RT for 1 hour. Subsequently, cell climbing slices were washed with PBS 3 times and further counterstained with DAPI for 3 minutes. Results were visualized under a fluorescence microscope (DM400B; Leica, Wetzlar, Germany).

RNA Isolation and Quantitative Real-Time PCR . Analysis was carried out by quantitative real-time PCR (qRT-PCR) to identify any the corneal alkali burn and cell changes upon the FDI-6 treatment. Corneal tissues were harvested at day 7 post-alkali burn and murine macrophages (RAW264.7 cells) were collected 24 hours after treatment. Then, total RNA from corneas or cells was extracted with Trizol Reagent (Invitrogen, Carlsbad, CA, USA) and reverse transcribed into cDNA using a kit (RevertAid First Strand cDNA Synthesis Kit; Thermo Fisher Scientific, Pittsburgh, PA, USA). The qRT-PCR was performed using SYBR Green Real-Time PCR Master Mix (Toyobo, Osaka, Japan). Results were calculated by the $2^{-\Delta\Delta Ct}$ method and normalized to GAPDH. The primers used in this study are listed as follows: Rat primers: CD31 sense, GGACTGCGCCCATCACTTACC; and antisense, AACTTCATCCACCGG GGCTATTAC; VEGF sense, GTCCTCACTTGGATCCCGACA; antisense, CCTGG CAGGCAAACAGACTTC; MMP-9 sense, AACTCAGCCTTTGAGGATCC; antisense, CAG TAT CCA GTG CAT CCG GT; endothelial NO synthase (eNOS) sense, CTTTCGGAAGGCGTTTGAC; antisense, AACTCTTGTGCTGCTCAGG; fibronectin (FN) sense, ATGATGGCAGAACACCCGC; antisense, TGCTGTGTTCC ATCTGCACT; α-SMA sense, ACTGGGACGACATGGAAAAG; antisense, CATCT CCAGAGTCCAGCACA; interleukin-6 (IL-6) sense, GTCAACTCCATCTGCCCTT CAG; antisense, GGCAGTGGCTGTCAACAACAT; FOXM1 sense, TCACAACCT TTCTCTCCATGAC; antisense, CCTGGTTCCAGTGGCTTAAA; GAPDH sense, TCCTGCACCACCAACTGCTTAG; antisense, AGTGGCAGTGATGGCATGGAC T; Mouse primers: monocyte chemotactic protein-1 (MCP-1) sense, TTAAAAACCT GGATCGGAACCAA; antisense, GCATTAGCTTCAGATTTACGGGT; interleukin-1β (IL-1β) sense, TTCAGGCAGGCAGTATCACTC; antisense, GAAGGTCCACGG GAAAGACAC; tumor necrosis factor-alpha (TNF-α) sense, CAGGCGGTGCCTAT GTCTC; antisense, CGATCACCCCGAAGTTCAGTAG; nucleotide-binding oligomerization domain-like receptor family pyrin domain-containing 3 (NLRP3) sense, ATCAACAGGCGAGACCTCTG; antisense, GTCCTCCTGGCATACCATAGA; VEGFA sense, GCACATAGAGAGAATGAGCTTCC; antisense, CTCCGCTCTGA ACAAGGCT; GAPDH sense TGACCTCAACTACATGGTCTACA; and antisense, CTT CCCATTCTCGGCCTTG.

Western Blot. Western Blot analysis was carried out to quantify the expression levels of FOXM1, FN, α-SMA, MMP-9, VEGFA, eNOS, phospho-endothelial NO synthase (p-eNOS), and RhoA. Corneal tissues were harvested at day 7 post-alkali burn and MRMECs seeded in 6-well plates were collected 24 hours after treatment. Then, total proteins were extracted from corneas or cells using radioimmunoprecipitation assay (RIPA) lysis buffer (CWBio, Beijing, China) containing 1% protease inhibitor cocktail (Sigma Aldrich). Equal amounts of protein (20 µg) were fractioned in a commercial polyacrylamide gel (Bio-Rad, Hercules, CA, USA) and transferred to PVDF membranes, followed by blocking in 5% skim milk for 1 hour. Subsequently, membranes were incubated with the following primary antibodies: FOXM1, FN (ab6328; Abcam, Cambridge, MA, USA), α-SMA (ab7817; Abcam), MMP-9 (ab76003; Abcam), VEGFA (ab214424; Abcam), eNOS (32027; Cell Signaling Technology, Danvers, MA, USA), p-eNOS (9574; Cell Signaling Technology), and RhoA (2117, rabbit monoclonal antibody, 1:1,000; Cell Signaling Technology) overnight at 4°C, followed by incubation with corresponding secondary antibodies (1:10000; ZSGB-Bio) for 1 hour at RT. Finally, bands were visualized using enhanced chemiluminescence (92-14860-00; ProteinSimple, San Jose, CA, USA) and analyzed by ImageJ software (National Institutes of Health [NIH], Bethesda, MD, USA).

Cell Culture

Given the fact that alkali-induced corneal NV has been mainly associated with the corneal infiltration of inflammatory cells (e.g. macrophages or neutrophils),[8] an LPS-induced RAW264.7 cell model was established to explore the anti-inflammatory activity of FDI-6. The critical roles of ECs in the formation of corneal NV,[10] which includes cell proliferation, migration, and tube formation, were analyzed to assess the antiangiogenic effect of FDI-6 in MRMECs. The MRMECs and RAW264.7 cells were purchased from Saibaikang Biotechnology Co. (Shanghai, China) and cultivated at 37°C in a 5% CO_2 incubator in different culture systems (MRMECs: PriMed-iCell-002, iCell Bioscience Inc., Shanghai; RAW264.7 cells: iCell-m047-001b, iCell Bioscience Inc.) which were replaced once a day. Cells at passage 3 to 6 were used in this study.

Cytotoxicity and Cell Proliferation Assay. The biological activity of FDI-6 was evaluated in MRMECs and RAW264.7 cells in terms of its cytotoxic and anti-proliferative ability. MRMECs (3000 cells/well) were seeded in 96-well plates with growth medium for 12 hours and further treated with FDI-6 at various concentrations (0, 1, 2.5, 5, 10, 20, 30, 40, and 60 µM for cytotoxicity assay and 0, 1, 2.5, 5, 10, and 20 µM for cell proliferation assay) for 24 hours. RAW264.7 (3000 cells/well) cells were seeded in 96-well plates with growth medium for 12 hours and further treated with FDI-6 at various concentrations (0, 2.5, 5, 10, 20, 40, and 60 µM for cell proliferation and cytotoxicity and assay) in the presence of LPS (1 µg /mL) for 24 hours. Cytotoxicity was detected using CytoTox96 LDH release kit (Promega, Fitchburg, WI, USA) and cell proliferation was determined using the Cell Counting Kit-8 (Dojindo Laboratories, Kumamoto, Japan) according to the manufacturer's instructions.

Migration Assay. To assess the effect of FDI-6 on cell migration, MRMECs (4500 cells/well) were seeded in 24-well plates with growth medium for 24 hours. Then, the plates were scratched with the tip of the sterilized 200 µL pipette when the cells reached about 80% to 90% confluence. After washing the debris, MRMECs were treated with FDI-6 diluted in serum-free medium for 24 hours, and images were finally taken at 0, 12, and 24 hours, respectively. The percentage of wound healing was calculated with the following formula: % wound healing = (initial wound area − unhealed wound area) / initial wound area × 100, and were analyzed using ImageJ software.[26]

Tube Formation Assay. To analyze the effect of FDI-6 on tube formation, MRMECs (4×10^4 cells/well) were seeded in 48-well plates that were pre-coated with basement membrane matrix (30 µl/well; Corning Incorporated, Corning, NY, USA) and treated with FDI-6 in a depleted medium for 12 hours. Images were captured under a microscope, and the number (Nb) of mesh tubes and nodes was finally assessed using ImageJ software.

Statistical Analysis

All data were analyzed using SPSS 22 software (IBM-SPSS, Chicago, IL, USA). Paired Student's *t*-test was used to calculate the significance of differences between the two groups. One-way analysis of variance (ANOVA) was used for comparison among three or more groups, followed by Tukey post hoc test for homogeneous variances or Tamhane's T2 post hoc test for non-homogeneous variances. A P value < 0.05 was considered statistically significant. All data were shown as the mean ± standard error of the mean (SEM), and all charts were created using GraphPad Prism 6.0 software.

Results

FDI-6 Suppressed Corneal NV and Inflammation in an Alkali Burn Injury Rat Model In Vivo

FDI-6 is a specific inhibitor of FOXM1 that has been shown to exert antiangiogenic and anti-inflammatory properties in previous studies.[14] To determine the role of FDI-6 (40 µM) in inflammatory corneal NV in vivo, a corneal alkali burn model was established in SD rats. As shown in Figure 1A, from day 1 to day 4 post-alkali burn, the corneas in the saline + and the FDI-6 + burn groups exhibited significant edema and corneal opacity, which was attenuated in the FDI-6 + burn group at day 7 post-alkali burn (corneal edema, $P < 0.01$; Fig. 1B; and corneal opacity, $P < 0.001$; Fig. 1C). Moreover, the inflammatory index exhibited a slight decrease from day 1 to day 7 in the saline + burn group and a dramatic decrease in the FDI-6 + burn group at day 7 ($P < 0.01$; Fig. 1D). Furthermore, an ingrowth of new blood vessels from the limbal plexus into the central cornea was observed from day 1 to day 7 post-alkali burn, whereas the area and the average length of corneal NV in the FDI-6 + burn group were significantly decreased at day 7 post-alkali burn compared with the saline + burn group ($P < 0.01$; Figs. 1F, 1G). In addition, a positive fluorescein staining was observed in the central cornea of rats from the saline + burn group at day 7 post-alkali burn, indicating the presence of corneal epithelial defects, whereas a negative fluorescein staining was observed in peripheral cornea of rats from the FDI-6 + burn group. Consistently, the corneal fluorescein staining scores also indicated a significant difference between the two groups mentioned above at day 7 ($P < 0.05$; see Fig. 1E). These results suggest that topical application of FDI-6 can significantly inhibit alkali burn-induced corneal NV and inflammation.

FDI-6 Attenuated Corneal NV and Fibrosis Induced by Alkali Burn

Corneal injury caused by alkali burn can result in corneal NV and subsequent fibrosis, ultimately leading to corneal opacification and visual impairment.[27] To examine the effects of FDI-6 on corneal NV and fibrosis induced by alkali burn ex vivo, each group was compared by H&E staining, Masson's trichrome staining, and immunochemical staining of α-SMA, CD31, and FOXM1 at day 7 post-alkali burn. As shown in Figures 2A and 2B, the average corneal thickness was significantly increased in the saline + burn group ($P < 0.001$) compared with the saline-only group, whereas it was significantly decreased in the FDI-6 + burn group ($P < 0.01$). Masson's trichrome staining also showed a significant increase and a decline in corneal stroma fibrosis in the saline + burn group ($P < 0.001$) and the FDI-6 + burn group ($P < 0.05$; see Figs. 2A, 2C), respectively. Moreover, the protein expression of α-SMA, a key marker of myofibroblasts in the corneal stroma was increased after alkali injury and decreased after FDI-6 treatment (see Fig. 2A). Furthermore, immunohistochemical staining of CD31, a specific marker of ECs, showed an increased and decreased number of CD31-positive structures surrounding a lumen in the saline + burn group ($P < 0.01$; see Figs. 2A, 2D) and the FDI-6 + burn group ($P < 0.05$; see Figs. 2A, 2D), respectively. Additionally, FOXM1 protein was mainly upregulated in the vessel wall and fibroblasts after alkali injury and was downregulated following topical application of FDI-6 (see Fig. 2A). These results indicate that topical application of FDI-6 can attenuate alkali burn-induced corneal NV and fibrosis.

FDI-6 Reduced Corneal Inflammatory Infiltration and Cellular Apoptosis Induced by Alkali Burn

Alkali burn can lead to significant corneal infiltration of inflammatory macrophages or neutrophils, ultimately playing a critical role in the development of corneal NV.[28] To further assess the effect of FDI-6 on the inflammatory response during alkali burn-induced corneal NV, immunofluorescence analysis of CD163 (a marker of type 2 macrophages) was conducted. As shown in Figure 3A,

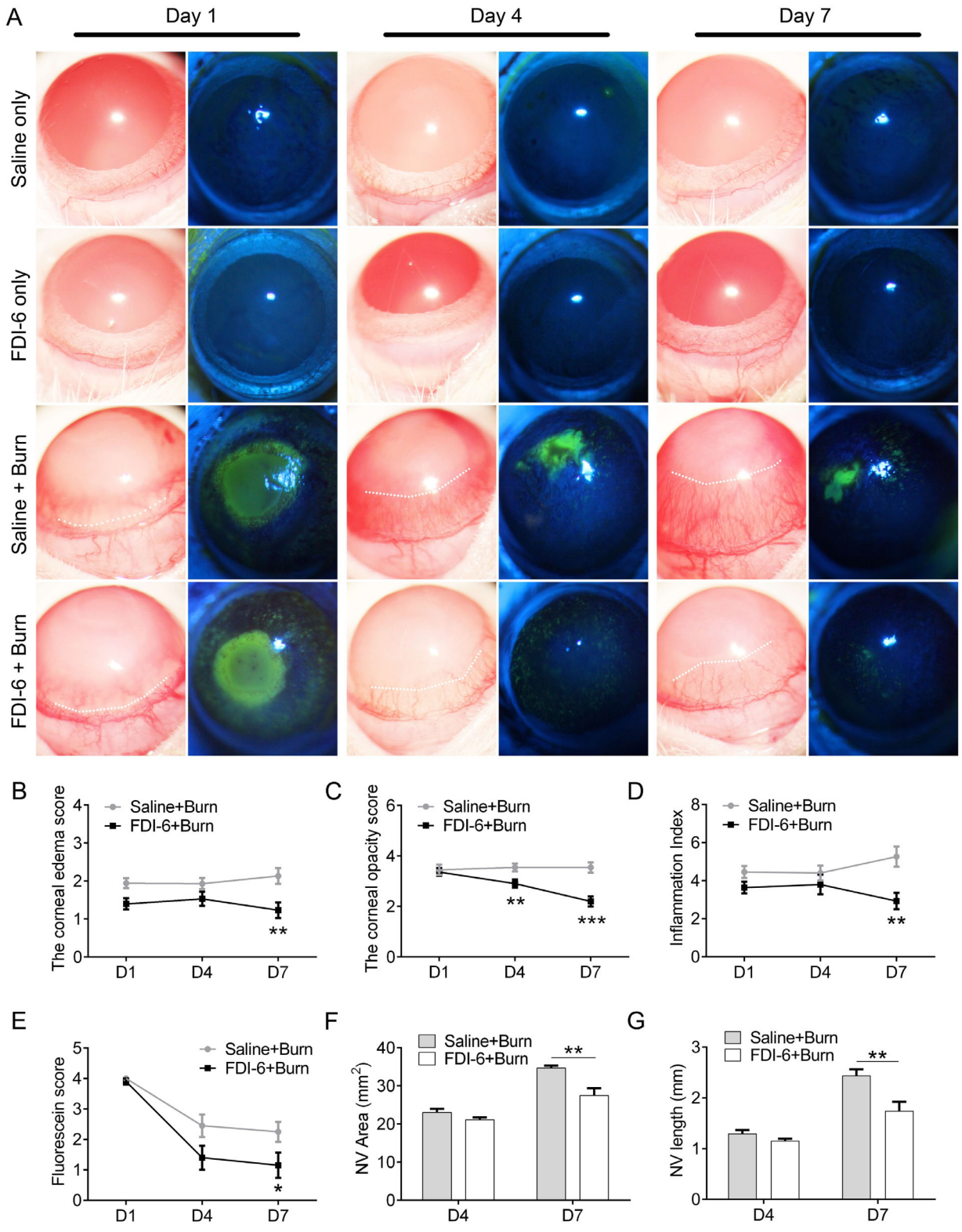

Figure 1. FDI-6 suppressed corneal NV and inflammation in an alkali-burn injury rat model in vivo. (**A**) Representative images of rat corneas under slit lamp showing differences in corneal NV and fluorescein staining among the groups on days 1, 4, and 7 after alkali burn; the dashed line (*white*) indicates the border between the vascularized and avascular area in corneas. (**B**) The corneal edema score on days 1, 4, and 7 in both groups ($N = 10$ per group). (**C**) The corneal opacity score on days 1, 4, and 7 in both groups ($N = 10$ per group). (**D**) Evaluation of inflammatory index of ocular surface on days 1, 4, and 7 in both groups ($N = 10$ per group). (**E**) Corneal fluorescein staining score on days 1, 4, and 7 in both groups ($N = 10$ per group). (**F, G**) Quantitative analysis of the area and the average length of new blood vessels on days 4 and 7 in both groups ($N = 14$ per group). $^{*}P < 0.05$, $^{**}P < 0.01$, the FDI-6 + burn group versus the saline + burn group. Results were shown as mean ± SEM.

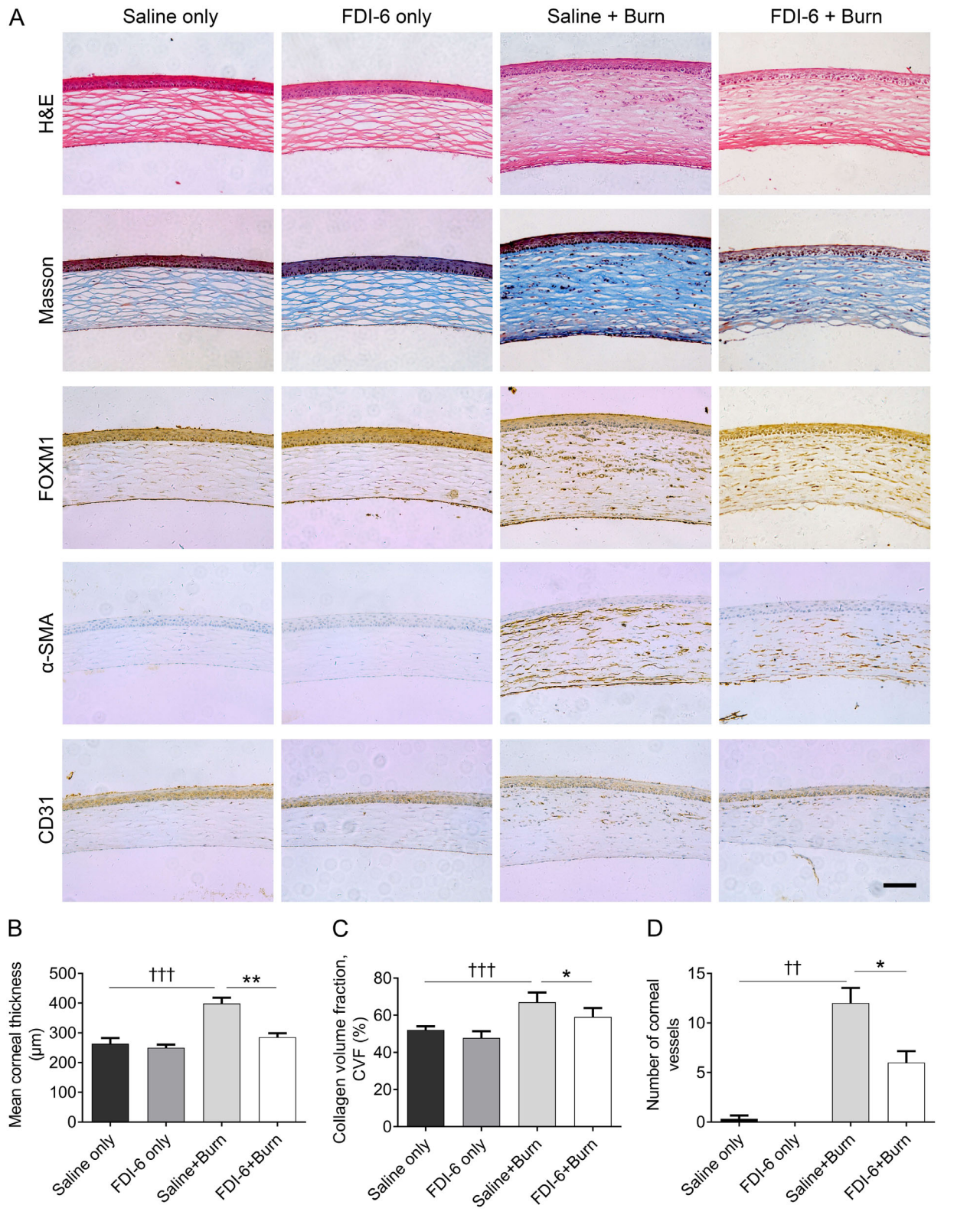

Figure 2. FDI-6 attenuated corneal NV and fibrosis induced by alkali burn. (**A**) Representative images of rat corneal sections stained with H&E, Masson's trichrome, and immunohistochemical staining of α-SMA, FOXM1, and CD31 in the different groups on day 7 after alkali burn. Quantitative analysis of the mean corneal thickness (**B**) ($N = 5$ per group), collagen volume fraction (**C**) ($N = 5$ per group), and the number of CD31-positive structures (**D**) ($N = 4$ per group). Scale bars: 100 μM. *$P < 0.05$ and **$P < 0.01$, the FDI-6 + burn group versus the saline + burn group; †$P < 0.001$, the saline + burn group versus the saline-only group. Results were shown as mean ± SEM.

Investigative Ophthalmology & Visual Science

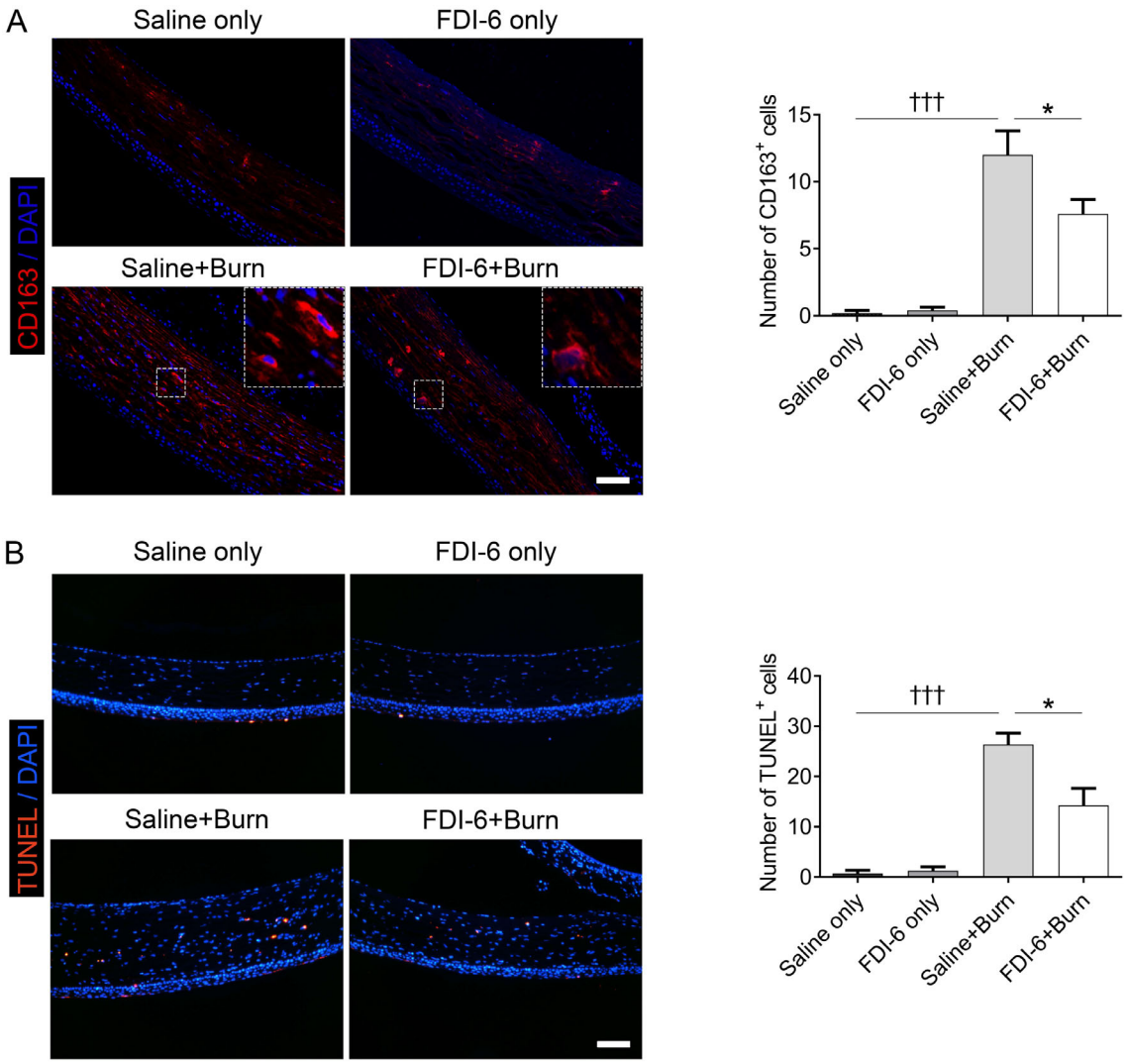

Figure 3. FDI-6 reduced corneal inflammatory infiltration and cellular apoptosis induced by alkali burn. (**A**) Representative images of corneal immunofluorescence staining of CD163 and quantitative analysis of the number of CD163+ cells among the groups on day 7 after alkali burn. *Red*: CD163-positive cells and *blue*: DAPI. The *white* boxes are shown as enlarged images. Scale bars: 100 µM. (**B**) Representative images of corneal TUNEL staining and quantitative analysis of the number of TUNEL+ cells among the groups on day 7 after alkali burn. *Red*: TUNEL-positive cells and *blue*: DAPI. Scale bars: 100 µM. $N = 4$ per group. $^{*}P < 0.05$, the FDI-6 + burn group versus the saline + burn group; $^{\dagger\dagger\dagger}P < 0.001$, the saline + burn group versus the saline-only group. Results were shown as mean ± SEM.

there was no significant difference between the saline- and FDI-6-only groups ($P > 0.05$), indicating that FDI-6 did not induce an inflammatory response in healthy corneas. However, the number of CD163-positive cells mainly located in corneal stroma was significantly increased in the saline + burn group ($P < 0.001$) but was decreased in the FDI-6 + burn group ($P < 0.05$). These results indicate that FDI-6 can suppress macrophage infiltration into the alkali-injured corneas.

Furthermore, corneal inflammatory infiltration was promoted to a certain extent by excessive corneal apoptosis triggered by alkali burn-induced corneal epithelial or stroma damage.[29] To further assess whether FDI-6 exerts an anti-apoptotic effect, a TUNEL assay was performed. As shown in Figure 3B, no differences in the number of TUNEL-positive cells were found between the saline- and FDI-6-only groups ($P < 0.05$). However, numerous TUNEL-positive cells were significantly increased in the saline + burn group ($P < 0.001$) and decreased in the FDI-6 + burn group ($P < 0.05$). These results substantiate that topical application of FDI-6 can alleviate alkali burn-induced keratocyte apoptosis, and 40 µM of FDI-6 does not compromise the ocular surface health in vivo.

FDI-6 Downregulated the Expression of Genes Related to Neovascularization, Inflammation, and Fibrosis

The above results demonstrated that FDI-6 exhibits anti-neovascularization, anti-fibrosis, and anti-inflammation properties in the alkali-injured corneas. To further explore the molecular mechanisms underlying the effects of FDI-6, qRT-PCR and Western Blot were used to quantify the changes in mRNA and protein levels of angiogenic factors (VEGF, CD31, MMP-9, and eNOS), fibrotic factors (FN and

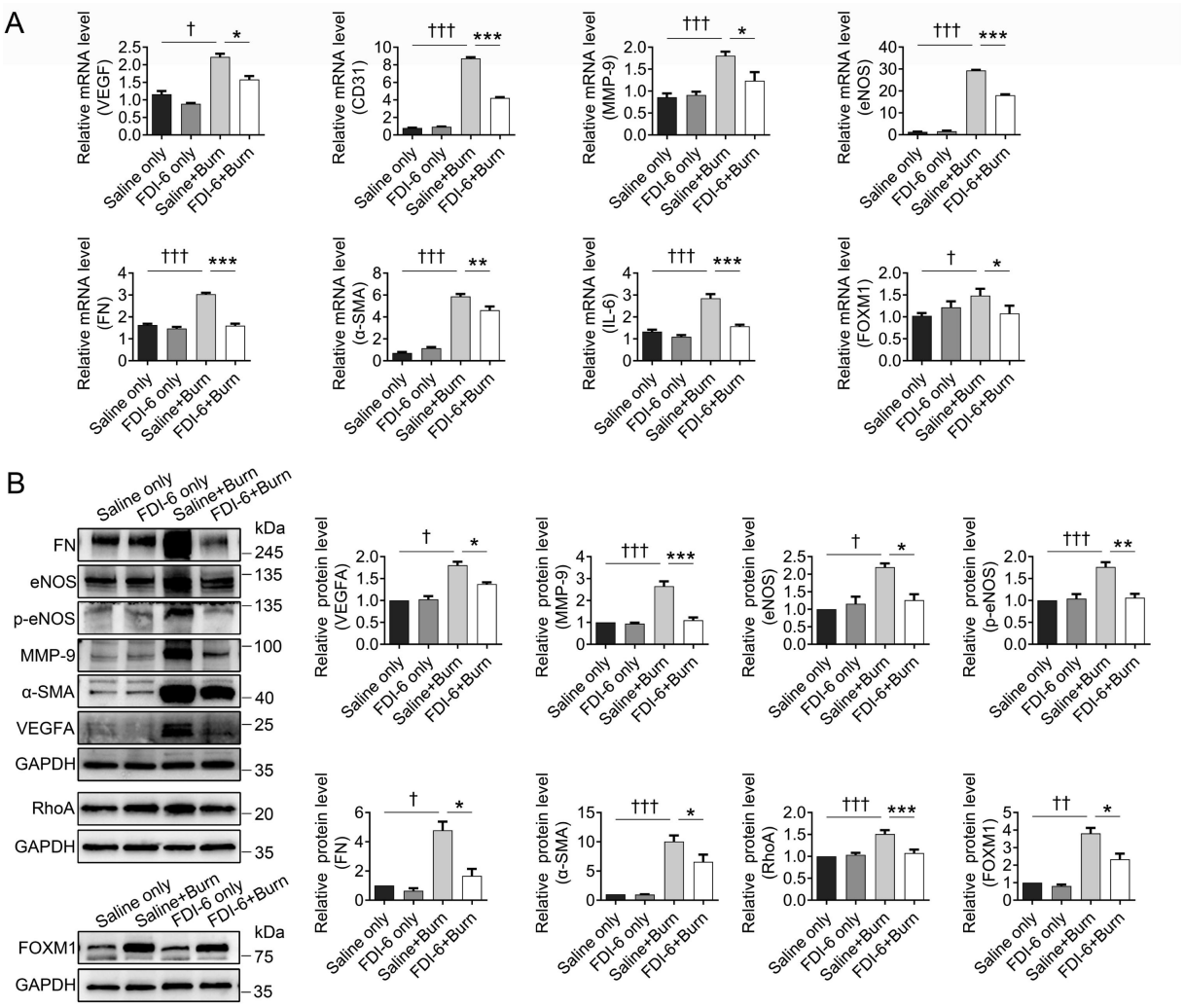

Figure 4. FDI-6 down-regulated the expression of genes related to neovascularization, inflammation, and fibrosis. (**A**) Quantitative analysis of mRNA expression of VEGF, CD31, MMP-9, eNOS, FN, α-SMA, IL-6, and FOXM1 among the groups on day 7 after alkali burn ($N = 4$ per group). (**B**) Western blot images and quantitative analysis of VEGFA, MMP-9, eNOS, P-eNOS, FN, α-SMA, FOXM1, and RhoA proteins among the groups on day 7 after alkali burn ($N = \geq 3$ per group). GAPDH was used as a loading control, and these values were further normalized to that value of the saline-only group. $^{*}P < 0.05$, $^{**}P < 0.01$, and $^{***}P < 0.001$, the FDI-6 + burn group versus the saline + burn group; $^{\dagger}P < 0.05$, $^{\dagger\dagger}P < 0.01$, and $^{\dagger\dagger\dagger}P < 0.001$, the saline + burn group versus the saline-only group. Results were shown as mean ± SEM.

α-SMA), pro-inflammatory factor (IL-6), and FOXM1 in alkali-injured corneas on day 7. As shown in Figure 4A, the mRNA levels of VEGF ($P < 0.05$), CD31 ($P < 0.001$), MMP-9 ($P < 0.001$), eNOS ($P < 0.001$), FN ($P < 0.001$), α-SMA ($P < 0.001$), IL-6 ($P < 0.001$), and FOXM1 ($P < 0.05$) in rat corneas were significantly increased in the saline + burn group compared with the saline-only group but were reduced in the FDI-6 + burn group (VEGF, $P < 0.05$; CD31, $P < 0.001$; MMP-9, $P < 0.05$; eNOS, $P < 0.001$; FN, $P < 0.001$; α-SMA, $P < 0.01$; IL-6, $P < 0.001$; and FOXM1, $P < 0.05$). Similarly, the protein levels of VEGF ($P < 0.05$), MMP-9 ($P < 0.001$), eNOS ($P < 0.05$), p-eNOS ($P < 0.001$), FN ($P < 0.05$), α-SMA ($P < 0.001$), and FOXM1 ($P < 0.01$) in rat corneas were upregulated in the saline + burn group compared with the saline-only group but were downregulated in the FDI-6 + burn group (VEGF, $P < 0.05$; MMP-9, $P < 0.001$; eNOS, $P < 0.05$; p-eNOS, $P < 0.01$; FN, $P < 0.05$; α-SMA, $P < 0.05$; IL-6, $P < 0.001$; and FOXM1, $P < 0.05$; Fig. 4B). Moreover, there were no significant differences in mRNA and protein expression between the saline- and FDI-6-only groups. In recent years, the RhoA/ROCK signaling pathway has been shown to play a critical role in angiogenesis.[30] As expected, RhoA protein expression was increased in the saline + burn group compared with the saline-only group ($P < 0.001$) and was decreased in the FDI-6 + burn group ($P < 0.001$; see Fig. 4B). These results indicate that topical application of FDI-6 can simultaneously downregulate the alkali-induced expression of angiogenic-, fibrotic-, and pro-inflammatory factors to a certain extent through the RhoA/ROCK signaling pathway.

FDI-6 Inactivated Growth of RAW264.7 Cells in Culture

To further identify whether FDI-6 alleviates alkali burn-induced corneal NV by inhibition of macrophage activation, a well-established model of LPS-stimulated RAW264.7 cells was used for all subsequent assessments. As seen in Figures 5A and 5B, FDI-6 induced cytotoxicity at concentrations exceeding 10 µM, and the cell proliferation was unaffected

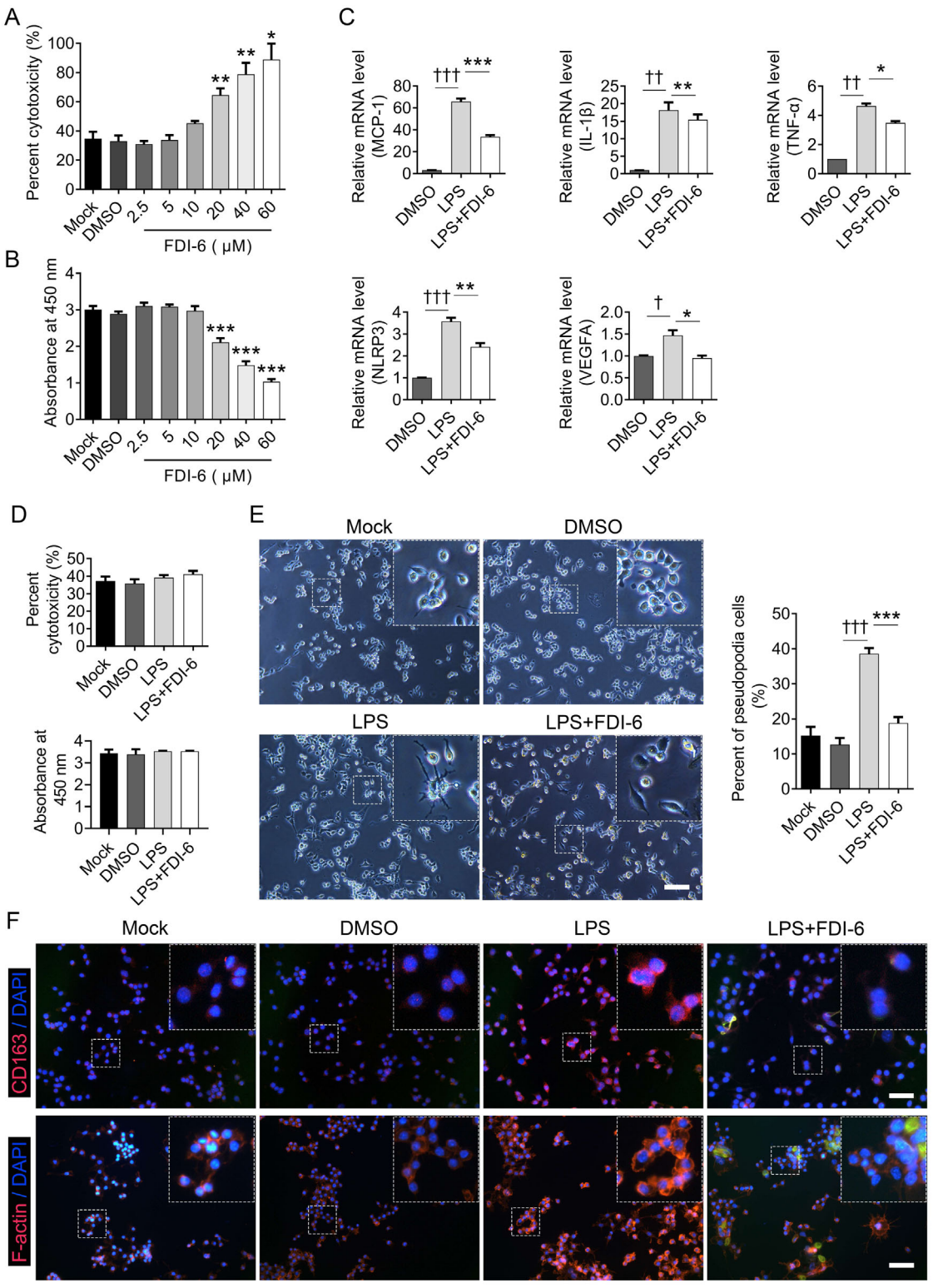

Figure 5. FDI-6 inactivated growth of RAW264.7 cells in culture. (**A**) Quantitative analysis of cell cytotoxicity of RAW264.7 cells treated with FDI-6 at various concentrations (0, 2.5, 5, 10, 20, 40, and 60 μM) for 24 hours (n [number of replicates] = 3 per group). (**B**) Quantitative analysis of cell proliferation of RAW264.7 cells treated with FDI-6 at various concentrations (0, 2.5, 5, 10, 20, 40, and 60 μM) for 24 hours (n = 3 per group). (**C**) Quantitative analysis of mRNA expression of MCP-1, IL-1β, TNF-α, NLRP3, and VEGFA in LPS-induced RAW264.7 cells pretreated with FDI-6 (10 μM) (n = 4 per group). (**D**) Quantitative analysis of cytotoxicity and cell proliferation in LPS-stimulated RAW264.7 cells pretreated with FDI-6 (10 μM) (n = 3 per group). (**E**) Representative images of cellar morphology in LPS-stimulated RAW264.7 cells pretreated with FDI-6 (10 μM) and quantitative analysis of the cells with filopodia (n = 4 per group). Scale bars: 100 μM. (**F**) Fluorescence micrographs of CD163 staining and F-actin staining of RAW264.7 cells pretreated with FDI-6 (10 μM). *Red*: CD163 or F-actin and *blue*: DAPI. Scale bars: 50 μM. *$P < 0.05$, **$P < 0.01$, and ***$P < 0.001$, the FDI-6 group versus the DMSO group (A, B) and the LPS + FDI-6 group versus the LPS group (C, E); $^{\dagger}P < 0.05$, $^{\dagger\dagger}P < 0.01$, and $^{\dagger\dagger\dagger}P < 0.001$, the LPS group versus the LPS group. Results were shown as mean ± SEM.

Investigative Ophthalmology & Visual Science

at concentrations of 0 to 10 µM and decreased at higher concentrations (>10 µM) of FDI-6. This finding suggested that 10 µM was the optimal concentration of FDI-6 for further experiments in RAW264.7 cells.

As shown in Figure 5D, LPS (1 µg/mL) or FDI-6 (10 µM) exerted no cell proliferation or cytotoxicity effects on RAW264.7 cells ($P > 0.05$). However, LPS-stimulated cells exhibited a larger number of long and slim pseudopodia

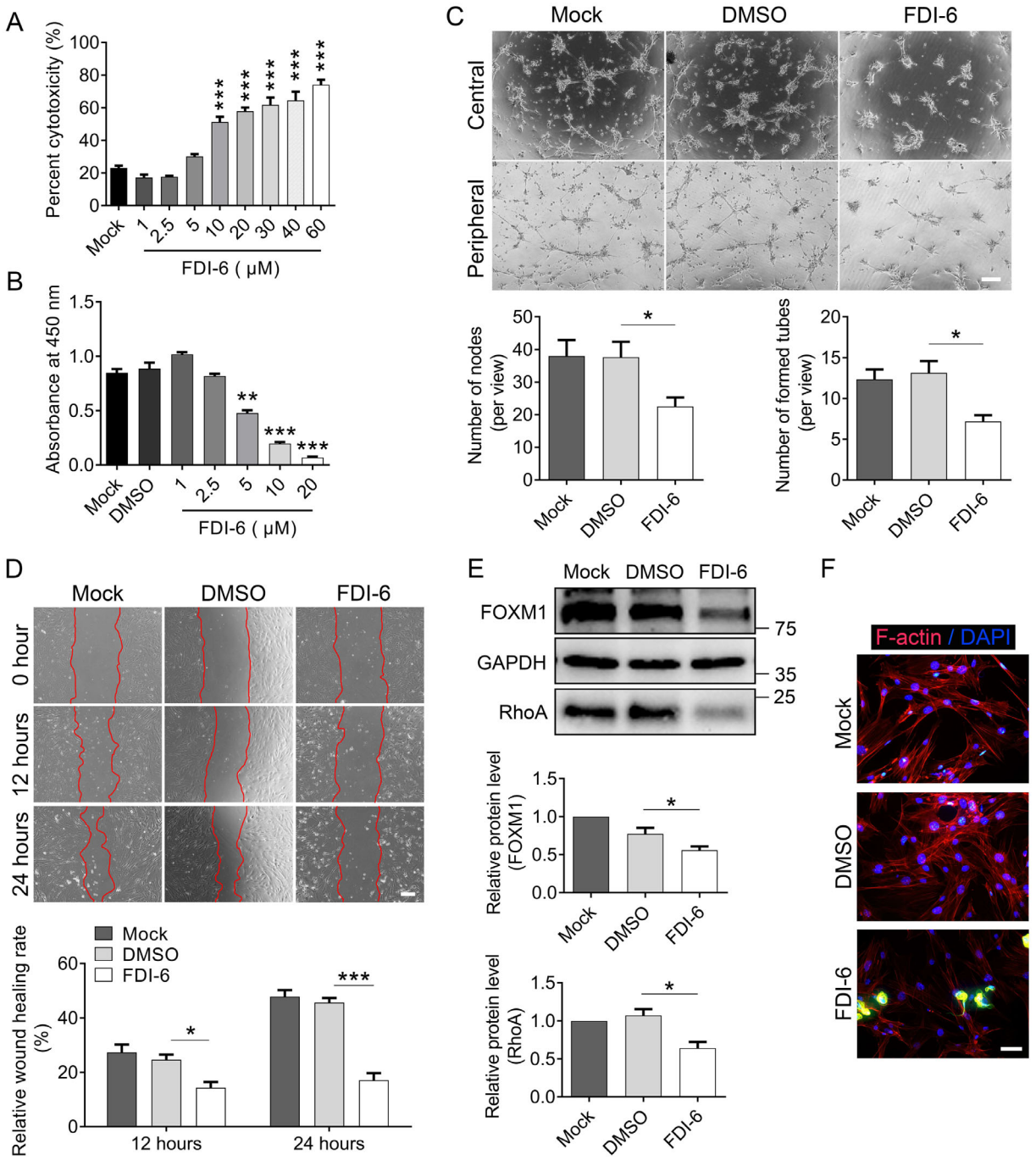

Figure 6. FDI-6 suppressed the proliferation, migration and tube formation of MRMECs in culture. (**A**) Quantitative analysis of cell cytotoxicity of MRMECs treated with FDI-6 at various concentrations (0, 1, 2.5, 5, 10, 20, 30, 40, and 60 µM) for 24 hours ($n = 3$ per group). (**B**) Quantitative analysis of cell proliferation of MRMECs treated with FDI-6 at various concentrations (0, 1, 2.5, 5, 10, and 20 µM) for 24 hours ($n = 3$ per group). (**C**) Representative images and quantitative analysis of tube formation of MRMECs at 12 hours following treatment with FDI-6 (5 µM) ($n = 3$ per group). Scale bars: 200 µM. (**D**) Representative images and quantitative analysis of scratch wound healing migration of MRMECs at 0 hour, 12 hours, and 24 hours following treatment with FDI-6 (5 µM) ($n = 3$ per group). The edges of the migrated cells were dotted with red lines. Scale bars: 200 µM. (**E**) Quantitative analysis of protein expression levels of RhoA and FOXM1 of MRMECs treated with FDI-6 (5 µM) ($n = 4$ per group). (**F**) Fluorescence micrographs of the F-actin cytoskeleton of MRMECs treated with FDI-6 (5 µM). *Red*: F-actin *blue*: DAPI; and *yellow*: residual FDI-6 particles. Scale bars: 200 µM. *$P < 0.05$, **$P < 0.01$, and ***$P < 0.001$, FDI-6 versus DMSO. Results were shown as mean ± SEM.

protrusions than the control cells (treated 0.04% DMSO; $P < 0.001$), which indicated that the cells were in an activated state. Subsequent addition of FDI-6 significantly reduced the number of these activated cells ($P < 0.001$; Fig. 5E). Moreover, there was an increase in the mRNA expressions of chemokines (MCP-1; $P < 0.001$), pro-inflammatory cytokines (IL-1β, $P < 0.01$ and TNF-α, $P < 0.01$), NLRP3 ($P < 0.001$), and VEGFA ($P < 0.05$) in LPS-stimulated cells. FDI-6 treatment resulted in significantly lower levels of these mRNA (MCP-1, $P < 0.001$; IL-1β, $P < 0.01$; TNF-α, $P < 0.05$; NLRP3, $P < 0.01$; and VEGFA, $P < 0.05$; Fig. 5C). In addition, immunofluorescent staining of CD163 also validated increased expression in LPS-stimulated cells, whereas FDI-6 decreased the LPS-induced high CD163 expression (Fig. 5F).

The RhoA/ROCK signaling pathway activity is responsible for its stimulatory effects on macrophage adhesion and inflammatory cytokine production.[31] As expected, LPS-stimulated cells exhibited enhanced fluorescence intensity of F-actin mainly regulated by RhoA, which was decreased by FDI-6 treatment (see Fig. 5F). These results indicate that FDI-6 can inhibit macrophage activation to a certain extent through the RhoA/ROCK pathway, ultimately attenuating alkali burn-induced corneal NV.

FDI-6 Suppressed the Proliferation, Migration and Tube Formation of MRMECs in Culture

The angiogenic process is closely linked to the activation, proliferation, migration, and tube formation of vascular endothelial cells.[32] Cultures of MRMECs treated with 0 to 60 µM of FDI-6 were assessed to explore whether FDI-6 could inhibit corneal NV by regulating the biological activities of MRMECs. As seen in Figure 6A, FDI-6 had no toxic effects on MRMECs at concentrations of 0 to 5 µM and induced cytotoxicity at concentrations of 10 to 60 µM. Thus, 5 µM of FDI-6 was used for further experiments of MRMECs in vitro.

To determine the effect of FDI-6 on the proliferation of MRMECs, cells were treated with 0 µM to 20 µM of FDI-6 (Fig. 6B). Consistent with the above observations, cell proliferation was inhibited in 5, 10, and 20 µM of FDI-6-treated cells compared with control (treated 0.02% DMSO) cells, and cells became ill-looking and started to die at 10 and 20 µM, suggesting cytotoxicity in MRMECs. Moreover, the migration area of MRMECs in 5 µM of FDI-6 treated cells was decreased at 12 hours ($P < 0.05$) and 24 hours ($P < 0.001$) after scratching compared with control cells (Fig. 6D). In addition, 5 µM of FDI-6 also inhibited the tube formation ability of MRMECs via a reduction in the number of tubes and nodes ($P < 0.05$; Fig. 6C).

It has been established that angiogenesis-associated processes, including cell migration and invasion, are also regulated by the RhoA/ROCK pathway.[30] Compared with control cells, the expression levels of RhoA and FOXM1 proteins were downregulated in 5 µM of FDI-6 treated cells ($P < 0.05$; Fig. 6E), whereas immunofluorescence of F-actin also showed a decreased expression in 5 µM of FDI-6 treated cells (Fig. 6F). These results indicate that FDI-6 is a potent inhibitor of the biological activities of ECs to a certain extent via the RhoA/ROCK pathway.

Discussion

Corneal neovascularization is a major risk factor responsible for corneal opacification and usually results from physical or chemical injuries. Corneal NV, which results from the imbalance between angiogenic and antiangiogenic molecules, can be attenuated by inhibiting of angiogenesis.[33] FOXM1 is a critical positive regulator of cell proliferation. Its overexpression can leading to excessive VEGF-A levels by directly or indirectly binding to the VEGF-A promoter region and promoting tumor angiogenesis in several cancers, including pancreatic cancer,[34] gastric cancer,[35] and glioma.[14] Moreover, knockdown of FOXM1 can reportedly suppress tumor angiogenesis through downregulation of pro-angiogenic factors, such as VEGF, MMP-2, or MMP-9. As a FOXM1 inhibitor, FDI-6 can bind directly to FOXM1, preventing FOXM1 from binding to its genomic target. FDI-6 has been reported to induce antitumor growth effect, involving decreased tumor angiogenesis via downregulation of FOXM1. However, a direct relationship between FDI-6 and angiogenesis has not been reported in the literature yet. In the current study, the effects of FDI-6 on alkali burn-induced corneal NV as well as fibrosis in a rat model were evaluated.

Our study showed that FDI-6 suppressed the rat corneal NV induced by alkali burn on day 7, resulting in a decline in CD31-positive vessels (a marker of ECs) in the cornea after FDI-6 treatment, consistent with the literature.[36,37] The antiangiogenic effect of FDI-6 was substantiated by the decreased expression of mRNA and protein of pro-angiogenic factors, including VEGF, MMP-9, and eNOS, that were upregulated in the chemically injured cornea. Furthermore, FOXM1, which is responsible for activation and recruitment of inflammatory cells, was inhibited by FDI-6, causing suppression of neutrophil and macrophage recruitment to the wound site, further delaying wound healing in diabetic foot ulcers.[38] Given that the essential role of inflammation in alkali-induced corneal NV has been established,[39] the effect of FDI-6 on inflammation was further explored. As expected, we found decreased inflammatory indexes on day 7 post-alkali burn for the FDI-6 treated corneas, whereas topical application of FDI-6 significantly reduced CD163-positive cells, which mainly infiltrated alkali-injured corneas during the chronic inflammatory stage. Interestingly, the inflammatory indexes were not decreased in the FDI-6-treated group 4 days after alkali burn injury, which accounted for the only inhibitory effect of FDI-6 on chronic inflammation and explained why corneal NV was not decreased in the FDI-6-treated group. It has been established that when the cornea is infiltrated by inflammatory cells, profibrotic cytokines are released to activate fibroblasts and initiate the fibrosis process.[40,41] FOXM1 is a key transcription factor regulating cell proliferation and survival, and its inhibition has been documented to attenuate tissue or organ fibrosis in many studies.[20,38] Consistently, topical application of FDI-6 markedly reduced alkali-induced expression of profibrotic factors, including FN and α-SMA at the mRNA and protein levels, which was further confirmed by Masson staining and immunohistochemical staining of α-SMA.

Previous studies demonstrated that macrophages play a critical role in the formation of corneal NV, and these tissue-infiltrating macrophages can further differentiate into alternatively activated type 2 macrophages that are proangiogenic and produce large amounts of chemotactic, proinflammatory, and proangiogenic cytokines.[42–44] Overexpression of MCP-1, a well-studied CC chemokine, can reportedly induce the recruitment of macrophages in corneal NV.[45] Moreover, pro-inflammatory cytokines (e, g. IL-1β, TNF-α, and VEGF-A) secreted by the activation of NLRP3

in monocytes can further modulate angiogenesis by interacting with angiogenic effectors cells.[46,47] In addition to the finding that FDI-6 inhibited macrophage infiltration into the alkali-injured corneas in vivo, the mRNA expression of chemokines (MCP-1), pro-inflammatory cytokines (IL-1β and TNF-α), NLRP3, and VEGFA was decreased by FDI-6 treatment in LPS-stimulated RAW264.7 cells in vitro. Moreover, the number of LPS-activated macrophage that exhibited filopodia was decreased, and CD163-positive cells (M2 macrophages) were reduced following FDI-6 treatment, which indicted that FDI-6 could suppress M2 macrophage polarization. These results indicate that FDI-6 inhibits the formation of corneal NV by inhibiting infiltrating inflammatory cells, such as macrophages and reducing the release of inflammation-related factors in macrophages.

It is well acknowledged that corneal NV is a complex process involving endothelial cell proliferation, migration, sprouting, and tube formation.[37,48] A previous study reported that knockdown of FOXM1 reduces human umbilical vein endothelial cell (HUVEC) proliferation,[14] and by targeting FOXM1, miR-34a-5p can attenuate LPS-induced HUVEC injury, excess proliferation, and tube formation.[49] In our present study, as a specific inhibitor of FOXM1, FDI-6 effectively suppressed the proliferation, migration, and tube formation of MRMECs in vitro, which accounted for the downregulation of VEGFA, MMP-9, and eNOS that were initially found to be upregulated in the alkali-induced cornea. Taken together, these results indicate that FDI-6 attenuates corneal NV by inhibiting the biological activities of vascular endothelial cells.

An increasing body of evidence suggests that the small GTPase RhoA and its downstream effector Rho kinase (ROCK) widely participate in angiogenesis (including ECs migration, proliferation, and tubulogenesis).[50–52] Moreover, the RhoA/ROCK pathway is reportedly a key mediator in several other inflammatory processes.[52] As a ROCK inhibitor, fasudil has been demonstrated to suppress alkali burn-induced corneal NV by decreasing inflammation and reducing ROS via the RhoA/ROCK pathway.[53] In our study, the RhoA protein was upregulated in alkali-injured corneas and was significantly downregulated by topical application of FDI-6 in vivo. The same tendency for RhoA expression was observed in LPS-induced RAW264.7 cells following treatment with FDI-6 in vitro. As previously described, the RhoA/ROCK pathway regulated the actin cytoskeleton and cell function.[52] The labeled F-actin fluorescence intensity was consistently decreased in LPS-induced RAW264.7 cells and MRMECs pretreated with FDI-6. These results corroborated that FDI-6 may affect corneal NV by regulating the RhoA/ROCK pathway.

With regard to safety, many adverse side effects of the agents commonly used in corneal NV, such as steroid-related glaucoma, cataract,[54] anti-VEGF drugs-related persistent epithelial defects, and delayed CWH,[55] were not observed in FDI-6 treated eyes. Conversely, corneal fluorescein staining demonstrated that topical application of FDI-6 did not cause any injury to corneas in the FDI-6 only group but instead promoted corneal wound healing in the FDI-6 + burn group in vivo. Moreover, no TUNEL-positive cells were observed in the FDI-6-only group, whereas a decrease in the number of TUNEL-positive cells was found in the FDI-6 + burn group. The histological analysis also showed an intact ocular surface structure in the FDI-6-only group. Accordingly, topical application of FDI-6 is safe and effective for the treatment of corneal NV. As a limitation of this research, the experiments were conducted for only 7 days because of an anticipated spontaneous regression of corneal NV and sclerosis of the remaining vessels described previously.[56] Accordingly, longer observation times are needed to investigate the antiangiogenic effects of FDI-6 and its other potential side effects.

In summary, our study demonstrated that FDI-6 simultaneously attenuates inflammation, neovascularization, and fibrosis in the cornea after alkali burn, with the inhibition of activated inflammatory cells and/or increased ECs activity, mediated to a certain extent by the RhoA/ROCK pathway. Because corneal NV is a complex and multistage pathological process, the multidimensional features of FDI-6 may shed new light on the treatment of corneal NV and other angiogenesis-related diseases.

Acknowledgments

Supported in part by the National Natural Science Foundation of China (82070928 [M.Y.], 81900829 [J.T.], 81770924 [X.L.], and 81970789 [Y.Z.]); the Department of Science and Technology of Sichuan Province (2020YJ0460 [M.Y.]); and the Sichuan Provincial Health Committee (19PJ117 [M.Y.]).

Disclosure: **C. Lan,** None; **G. Liu,** None; **L. Huang,** None; **X. Wang,** None; **J. Tan,** None; **Y. Wang,** None; **N. Fan,** None; **Y. Zhu,** None; **M. Yu,** None; **X. Liu,** None

References

1. Shakiba Y, Mansouri K, Arshadi D, Rezaei N. Corneal neovascularization: molecular events and therapeutic options. *Recent Pat Inflamm Allergy Drug Discov.* 2009;3(3):221–231.
2. Cursiefen C, Lu C, Borges LP, et al. VEGF-A stimulates lymphangiogenesis and hemangiogenesis in inflammatory neovascularization via macrophage recruitment. *J Clin Invest.* 2004;113:1040–1050.
3. Su W, Li Z, Li Y, et al. Doxycycline enhances the inhibitory effects of bevacizumab on corneal neovascularization and prevents its side effects. *Invest Ophthalmol Vis Sci.* 2011;52:9108–9115.
4. Lim P, Fuchsluger TA, Jurkunas UV. Limbal Stem Cell Deficiency and Corneal Neovascularization. *Semin Ophthalmol.* 2009;24:139–148.
5. Oh SY, Choi JS, Kim EJ, Chuck RS, Park CY. The role of macrophage migration inhibitory factor in ocular surface disease pathogenesis after chemical burn in the murine eye. *Mol Vis.* 2010;16:2402–2411.
6. Wang X, Tang L, Zhang Z, Li W, Chen Y. Keratocytes promote corneal neovascularization through VEGFr3 induced by PPARα-inhibition. *Exp Eye Res.* 2020;193:107982.
7. Andrés G, Leali D, Mitola S, et al. A pro-inflammatory signature mediates FGF2-induced angiogenesis. *J Cell Mol Med.* 2009;13:2083–2108.
8. Nominato L, Dias A, Dias L, et al. Prevention of Corneal Neovascularization by Adenovirus Encoding Human Vascular Endothelial Growth Factor Soluble Receptor (s-VEGFR1) in Lacrimal Gland. *Invest Ophthalmol Vis Sci.* 2018;59:6036–6044.
9. Maddula S, Davis D, Maddula S, Burrow M, Ambati BK. Horizons in therapy for corneal angiogenesis. *Ophthalmology.* 2011;118:591–599.
10. Chi Z, Melendez AJ.. Role of cell adhesion molecules and immune-cell migration in the initiation, onset and development of atherosclerosis. *Cell Adhesion & Migration.* 2007;1:171–175.

11. Gerber HP, Ferrara N. Pharmacology and Pharmacodynamics of Bevacizumab as Monotherapy or in Combination with Cytotoxic Therapy in Preclinical Studies. *Cancer Res.* 2005;65:671–680.
12. Jain RK. Antiangiogenesis strategies revisited: from starving tumors to alleviating hypoxia. *Cancer Cell.* 2014;26:605–622.
13. Gormally M, Dexheimer T, Marsico G, et al. Suppression of the FOXM1 transcriptional programme via novel small molecule inhibition. *Nat Commun.* 2014;5:5165.
14. Zhang Y, Zhang N, Dai B, et al. FoxM1B transcriptionally regulates vascular endothelial growth factor expression and promotes the angiogenesis and growth of glioma cells. *Cancer Res.* 2008;68:8733–8742.
15. Balli D, Ren X, Chou F, et al. Foxm1 transcription factor is required for macrophage migration during lung inflammation and tumor formation. *Oncogene.* 2012;31:3875–3888.
16. Zeng R, Lu X, Lin J, et al. FOXM1 activates JAK1/STAT3 pathway in human osteoarthritis cartilage cell inflammatory reaction. *Exp Biol Med.* 2021;246:644–653.
17. Kurahashi T, Yoshida Y, Ogura S, et al. Forkhead Box M1 Transcription Factor Drives Liver Inflammation Linking to Hepatocarcinogenesis in Mice. *Cell Mol Gastroenterol Hepatol.* 2020;9:425–446.
18. Goda C, Balli D, Black M, et al. Loss of FOXM1 in macrophages promotes pulmonary fibrosis by activating p38 MAPK signaling pathway. *PLoS Genet.* 2020;16:e1008692.
19. Xie H, Miao N, Xu D, et al. FoxM1 promotes Wnt/β-catenin pathway activation and renal fibrosis via transcriptionally regulating multi-Wnts expressions. *J Cell Mol Med.* 2021;25:1958–1971.
20. Lan C, Tan J, Tang L, et al. Forkhead domain inhibitory-6 attenuates subconjunctival fibrosis in rabbit model with trabeculectomy. *Exp Eye Res.* 2021;210:108725.
21. Ulhaka K, Kanokwiroon K, Khongkow M, Bissanum R, Khunpitak T, Khongkow P. The Anticancer Effects of FDI-6, a FOXM1 Inhibitor, on Triple Negative Breast Cancer. *Int J Mol Sci.* 2021;22:6685.
22. Li Y, Lu L, Tu J, et al. Reciprocal Regulation Between Forkhead Box M1/NF-κB and Methionine Adenosyltransferase 1A Drives Liver Cancer. *Hepatology.* 2020;72:1682–1700.
23. D'Amato RJ, Loughnan MS, Flynn E, Folkman JJR. Thalidomide Is an Inhibitor of Angiogenesis. *Retina.* 1996;16:268.
24. Laria C, Alió J, Ruiz-Moreno JM. Combined non-steroidal therapy in experimental corneal injury. *Ophthalmic Res.* 1997;29:145–153.
25. Guan J, Zhou L, Wang L, Li X, Z Pan. Germinal peptide eye drops promote corneal wound healing and decrease inflammation after alkali injury. *Exp Eye Res.* 2020;199:108191.
26. Santos J, Camões S, Filipe E, et al. Three-dimensional spheroid cell culture of umbilical cord tissue-derived mesenchymal stromal cells leads to enhanced paracrine induction of wound healing. *Stem Cell Res Ther.* 2015;6:90.
27. Bian F, Pelegrino F, Henriksson J, et al. Differential Effects of Dexamethasone and Doxycycline on Inflammation and MMP Production in Murine Alkali-Burned Corneas Associated with Dry Eye. *Ocul Surf.* 2016;14:242–254.
28. Yamada J, Dana M, Sotozono C, S Kinoshita. Local suppression of IL-1 by receptor antagonist in the rat model of corneal alkali injury. *Exp Eye Res.* 2003;76:161–167.
29. Wilson S, Chaurasia S, Medeiros FW. Apoptosis in the initiation, modulation and termination of the corneal wound healing response. *Exp Eye Res.* 2007;85:305–311.
30. Hyvelin J, Howell K, Nichol A, Costello C, Preston R, McLoughlin P. Inhibition of Rho-kinase attenuates hypoxia-induced angiogenesis in the pulmonary circulation. *Circ Res.* 2005;97:185–191.
31. Cheng C, Chen P, Lin Y, Kao YH. High glucose activates Raw264.7 macrophages through RhoA kinase-mediated signaling pathway. *Cell Signal.* 2015;27:283–292.
32. Chang J, Huang Y, Cunningham C, et al. Matrix metalloproteinase 14 modulates signal transduction and angiogenesis in the cornea. *Surv Ophthalmol.* 2016;61:478–497.
33. Ferrari G, Hajrasouliha AR, Sadrai Z, Ueno H, Chauhan SK, Dana R. Nerves and Neovessels Inhibit Each Other in the Cornea. *Invest Ophthalmol Vis Sci.* 2013;54:813–820.
34. [No authors listed]. Retraction: Down-regulation of Forkhead Box M1 Transcription Factor Leads to the Inhibition of Invasion and Angiogenesis of Pancreatic Cancer Cells. *Cancer Res.* 2018;78:5470.
35 Li Q, Zhang N, Jia Z, et al . Critical Role and Regulation of Transcription Factor FoxM1 in Human Gastric Cancer Angiogenesis and Progression. *Cancer Res.* 2009;69:3501–3509.
36. Han Y, Shao Y, Lin Z, et al. Netrin-1 simultaneously suppresses corneal inflammation and neovascularization. *Invest Ophthalmol Vis Sci.* 2012;53:1285–1295.
37. Li Z, Chen J, Lei L, et al. Laquinimod Inhibits Inflammation-Induced Angiogenesis in the Cornea. *Front Med.* 2020;7:598056.
38. Sawaya A, Stone R, Brooks S, et al. Deregulated immune cell recruitment orchestrated by FOXM1 impairs human diabetic wound healing. *Nat Commun.* 2020;11:4678.
39. Maruyama K, Nakazawa T, Cursiefen C, et al. The maintenance of lymphatic vessels in the cornea is dependent on the presence of macrophages. *Invest Ophthalmol Vis Sci.* 2012;53:3145.
40. Saika S, Yamanaka O, Okada Y, Sumioka T. Modulation of Smad signaling by non-TGFβ components in myofibroblast generation during wound healing in corneal stroma. *Exp Eye Res.* 2016;142:40–48.
41. Wolf M, Clay S, Zheng S, Pan P, Chan MF. MMP12 Inhibits Corneal Neovascularization and Inflammation through Regulation of CCL2. *Invest Ophthalmol Vis Sci.* 2019;9:11579.
42. Wang Y, Gao Y, Huang Y, et al. The potential protective effects of miR-497 on corneal neovascularization are mediated via macrophage through the IL-6/STAT3/VEGF signaling pathway. *Int Immunopharmacol.* 2021;96:107745.
43. Yang Y, Liu F, Tang M, et al. Macrophage polarization in experimental and clinical choroidal neovascularization. *Prog Retin Eye Res.* 2016;6:30933.
44. Sunderktter C, Steinbrink K, Goebeler M, Bhardwaj R, Sorg CJ. Macrophages and angiogenesis. *J Leukoc Biol.* 1994;55.
45. Zhou Y, Yoshida S, Nakao S, et al. M2 Macrophages Enhance Pathological Neovascularization in the Mouse Model of Oxygen-Induced Retinopathy. *Invest Ophthalmol Vis Sci.* 2015;56:4767–4777.
46. Horwitz V, Dachir S, Cohen M, et al. Differential expression of corneal and limbal cytokines and chemokines throughout the clinical course of sulfur mustard induced ocular injury in the rabbit model. *Exp Eye Res.* 2018;177:145–152.
47. Place DE, Kanneganti TD. Recent advances in inflammasome biology. *Curr Opin Immunol.* 2017;50:32–38.
48. Makanya AN, Hlushchuk R, Djonov VG. Intussusceptive angiogenesis and its role in vascular morphogenesis, patterning, and remodeling. *Angiogenesis.* 2009;12:113.
49. Zhang F, Zheng W, Wang HJ. MiR-34a-5p inhibition attenuates LPS-induced endothelial cell injury by targeting FOXM1. *Eur Rev Med Pharmacol Sci.* 2020;24:10829–10838.
50. Hyvelin JM, Howell K, Nichol A, Costello CM, Preston RJ, McLoughlin P. Inhibition of Rho-Kinase Attenuates Hypoxia-Induced Angiogenesis in the Pulmonary Circulation. *Circ Res.* 2005;97:185–191.

Investigative Ophthalmology & Visual Science

51. Hoang MV, Whelan MC, Senger DR. Rho activity critically and selectively regulates endothelial cell organization during angiogenesis. *Proc Natl Acad Sci USA*. 2004;101(7):1874–1879.
52. Liu J, Wada Y, Katsura M, et al. Rho-Associated Coiled-Coil Kinase (ROCK) in Molecular Regulation of Angiogenesis. *Theranostics*. 2018;8:6053–6069.
53. Zeng P, Pi R, Li P, et al. Fasudil hydrochloride, a potent ROCK inhibitor, inhibits corneal neovascularization after alkali burns in mice. *Mol Vis*. 2015;21:688–698.
54. Zhang Y, Yu Y, Li G, Zhang X, Wu Z, L Lin. Bioadhesive glycosylated nanoformulations for extended trans-corneal drug delivery to suppress corneal neovascularization. *J Mater Chem B*. 2021;9:4190–4200.
55. Kim T, Chung JL, Hong JP, Min K, Seo KY, Kim EK . Bevacizumab Application Delays Epithelial Healing in Rabbit Cornea. *Invest Ophthalmol Vis Sci*. 2009;50:4653–4659.
56. Edelman J, Castro M, Wen Y.. Correlation of VEGF expression by leukocytes with the growth and regression of blood vessels in the rat cornea. *Invest Ophthalmol Vis Sci*. 1999;40:1112–1123.

Investigative Ophthalmology & Visual Science